Marine and Petroleum Geology 89 (2018) 58–67

Contents lists available at ScienceDirect

Marine and Petroleum Geology

journal homepage: www.elsevier.com/locate/marpetgeo

Research paper

Geological and geochemical characteristics of marine-continental transitional shale from the Upper Permian Longtan formation, Northwestern Guizhou, China

Wen Luo [a, b], Mingcai Hou [a, b, *], Xinchun Liu [a, b], Shuguang Huang [a, b], Hui Chao [a, b], Rui Zhang [a, b], Xiang Deng [c]

[a] State Key Laboratory of Oil and Gas Reservoir Geology and Exploitation(Chengdu University of Technology), Chengdu 610059, China
[b] Institute of Sedimentary Geology, Chengdu University of Technology, Chengdu 610059, China
[c] Shale Gas Evaluation and Exploitation Key Laboratory of Sichuan Province, Chengdu 610091, China

ARTICLE INFO

Article history:
Received 30 September 2016
Received in revised form
27 May 2017
Accepted 19 June 2017
Available online 20 June 2017

Keywords:
Marine-continental transitional facies
Longtan formation
Geochemical characteristics
Shale gas potential

ABSTRACT

Organic-rich shale deposited in a marine-continental transitional facies was well developed in the upper Yangtze area during the Late Permian. It is considered to contain a large amount of shale hydrocarbon resources. This paper takes the Upper Permian Longtan shale in the central Guizhou uplift as an example to characterize the transitional shale reservoir. Based on organic geochemistry data, X-ray diffraction (XRD) analysis, and scanning electron microscopy (SEM) observation, the geochemical characteristics of this transitional shale were systematically studied and the shale gas potential was investigated. The results indicate that the Longtan shale has fair to good hydrocarbon potential with high total organic carbon (TOC) and contains type III gas-prone organic matter. Its high thermal maturity favors the generation of gas (Ro, 1.10%–2.74%). XRD analyses show that the mineral components of the transitional shale are dominated by high clay content (58.7 wt%). The clay minerals are dominated by illite (44%) and mixed illite/smectite (43%). SEM observation shows that intra-particle pores, inter-particle pores and microfracture were well developed in the Longtan shale, which can provide reservoir space for the accumulation of shale gas. Organic matter pores appear rare due to its organic type. In summary, the Longtan shale has high organic content, high maturation, and high gas content, all of which demonstrate its great potential as a shale-gas resource. But the high clay content of the Longtan shale may be a challenge to shale-gas production.

1. Introduction

The remarkable success in the exploration and development of shale gas in the United States has stimulated a shale gas exploration boom worldwide. China has also been encouraged to dedicate great effort to develop shale gas (Curtis, 2002; Bowker, 2007; Jarvie et al., 2007; Tang et al., 2014; Dang et al., 2015). At present, significant breakthroughs have been achieved in marine shale in southern China, and progress has been made in terrestrial shale in northwestern China. For marine shale, the Fuling shale gas field has been discovered in the southeastern Sichuan Basin, and the Lower Silurian Longmaxi Formation has become an important gas-producing stratum (Guo and Liu, 2013; Gai et al., 2016). For terrestrial shale, some demonstration plays have been established and multiple wells have been drilled, some of which have achieved gas production (Tang et al., 2014; Jiang et al., 2014; Gao et al., 2016). However, compared to marine shale and terrestrial shale, the research and exploration on transitional shale are still weak (Guo et al., 2014). In fact, transitional shales are distributed widely in China, such as the Carboniferous Benxi Formation and the Lower Permian Shanxi Formation-Taiyuan Formation in the Ordos Basin, the Carboniferous-Permian in the Junggar Basin, the Carboniferous-Permian in the Tarim Basin, and the Permian Longtan Formation in southern China. These shales are associated with coal and sandstones generally having high organic content and exhibit high maturity, with a relatively large cumulative thickness, and are considered to possess tremendous potential for shale gas

* Corresponding author. Institute of Sedimentary Geology, Chengdu University of Technology, 1#, Dongsanlu, Erxianqiao, Chengdu 610059, Sichuan, China.
E-mail address: houmc@cdut.edu.cn (M. Hou).

http://dx.doi.org/10.1016/j.marpetgeo.2017.06.029
0264-8172/

exploration (Zhang et al., 2008, 2009; Zou et al., 2010).

Many sets of shale formations have been developed in Guizhou. Recently, many scholars have studied the marine black shale of the lower Cambrian Niutitang Formation and Lower Silurian Longmaxi formation. Important progresses have been achieved on the sedimentary environment, reservoir characteristics, and reservoir control condition of shale gas (He et al., 2011; Li et al., 2012). Because of the limited influences of the researches and developments of shale gas, studies on the typical marine-continental transitional Longtan shale are relatively scarce. Only few studies have been conducted on reservoir characteristics. The Xiye-1 well is located in the central region of northwestern Guizhou. During the process of drilling, the gas content ranges from 1.40 m^3/t to 19.60 m^3/t, which indicates that marine-continental transitional Longtan shale has great potential for shale gas and may be as important as marine shale (Wang et al., 2015). The success of shale gas exploration and development in the Longtan transitional shale can not only increase the production of shale gas, but also alleviate the enormous environmental pressure.

This study aims to provide valuable insight for the development of transitional shale in the future by integrating a geological survey of northwest Guizhou with the analytical results of outcrop samples and the latest downhole data. We utilize the analysis of total organic carbon (TOC), Rock-Eval pyrolysis, X-ray diffraction (XRD) and scanning electron microscopy (SEM), to determine the geochemical characteristics of transitional shale. These results provide an important basis for further study of the potential of shale gas resources in the Longtan Formation. Furthermore, this study provides valuable insight for the comprehensive evaluation of transitional shale gas resources.

2. Geological setting

Guizhou Province is located in the southern margin of the upper Yangtze plate. Tectonically, it can be subdivided into the following six major structural units from north to south: north of Yunnan-Guizhou depression; Wuling depression; central Guizhou uplift; southwestern Guizhou depression; southern Guizhou depression and Xuefeng uplift (Fig. 1) (Niu et al., 2007).

The study area is located in the central Guizhou uplift, which is mainly in northwestern Guizhou. From the Sinian to the Middle Triassic, there was no obvious orogenic movement in this area, and water lifting activities alone lead to an interactive epicontinental environment. From the Late Ordovician to the Upper Permian, central Guizhou was elevated during the Caledonian movement. It was then subject to long-term weathering and denudation, causing the absence of the Lower Permian strata in large parts of this region (Niu et al., 2007; Dou et al., 2012). A wide sea regression affected northwestern Guizhou during the Dongwu movement in the Late Permian. The sedimentary environment of this region changed from an epicontinental sea to a lagoon, swamp and delta due to seawater retreat in the NE direction (Fig. 2A) (Zhao et al., 2008). During this phase, Longtan Formation shales were widely deposited in this region. The Longtan Formation is dominated by fine-grained sediments, which consists of a relatively thin layer of shale, thin bedded sandstone, siltstone and coal seams, with a thickness ranging from 55 to 157 m (Fig. 2B).

3. Material and methods

3.1. Samples and preparation

In this study, 58 experimental samples were collected from outcrops and drilling cores for the evaluation of the geochemical characteristics of the Longtan shale; of these, 40 samples were collected from outcrops, while 18 samples were collected from the well ZK01. The sample locations are shown in Fig. 1. Analytical techniques, including TOC, Rock-Eval pyrolysis, kerogen maceral composition, XRD and SEM, were used to determine the geochemical characteristics of the Longtan shale. All analyses were performed at Keyuan Engineering Testing Center, Sichuan, China. Before analysis, all shale samples were pretreated to meet the requirements of the experiment. Basic sample properties are listed in Table 1.

3.2. Experiments

TOC was measured using a Leco CS-400 carbon/sulfur analyzer. Firstly, hydrochloric acid was used to remove inorganic carbon in samples. After drying, the de-carbonated samples were heated to 1200 °C under oxygen flow to convert the organic carbon into carbon dioxide.

Rock-Eval pyrolysis was performed using a YQ-V II A Rock-Eval instrument. Crushed samples (approximately 40–60 mg in mass with 80 mesh size) were heated at a programmed rate. Then, a flame ionization detector and a thermal conductivity detector were used to quantitatively detect the hydrogen and carbon dioxide emitted from the heated organic matter, respectively. The measured parameters include free oil or volatile hydrocarbon content (S1, mg HC/g rock), the remaining hydrocarbon generation potential (S2, mg HC/g rock), and the temperature at the S2 peak (T_{max}). The hydrogen index (HI) was calculated in this study by using a method described by Behar et al. (2001).

Vitrinite reflectance values were obtained using a microscope photometer instrument. Kerogen maceral composition was analyzed with a microscope for 22 samples under reflected and transmitted light. The type of organic matter was determined by the relative abundances of primary maceral groups. Mineral compositions were determined using an X-ray diffractometer. All of the samples were crushed into a fine powder and then analyzed with a Panalytical X'Pert PRO MPD X-ray diffractometer with Cu Kα radiation (45 kV, 35 mA) at a scan rates of 2°/min over an angular range of 2°–60°. The relative abundances of various mineral phases were determined by analyzing the diffraction patterns of minerals, and a quantitative assessment was performed.

The microscopic pores were observed using an FEI Quanta200F scanning electron microscope. All samples were approximately cut into chips and initially polished using dry emery paper, and they were then processed using an argon-ion-beam milling device and a conductive coating device before observation.

4. Results and discussion

4.1. Organic geochemical characteristics

4.1.1. Organic matter abundance

TOC is one of the most important indicators for shale to evaluate the hydrocarbon generation potential. TOC can also have a decisive influence on the gas-sorption capacity of the shale (Ross and Bustin, 2009). Higher organic carbon content implies higher hydrocarbon generation potential and better adsorption capacity for shale gas. Currently, the lower limit of TOC for commercial exploitation of shale gas is generally 2.0%.However, a few scholars suggested that the lower limit of TOC of shale with a high-maturity stage can be reduced to 1% (Hunt, 1979; Curtis, 2002; Jarvie et al., 2007; Zou et al., 2010). Table 1 lists the TOC values for all 56 shale samples from both outcrops and cores. TOC values of the Longtan shale samples are generally high and ranges widely from 0.35% to 26.99%, with an average of 5.34%. Approximately 71.4% of the TOC values exceed 2%, indicating that most samples could have fair to very

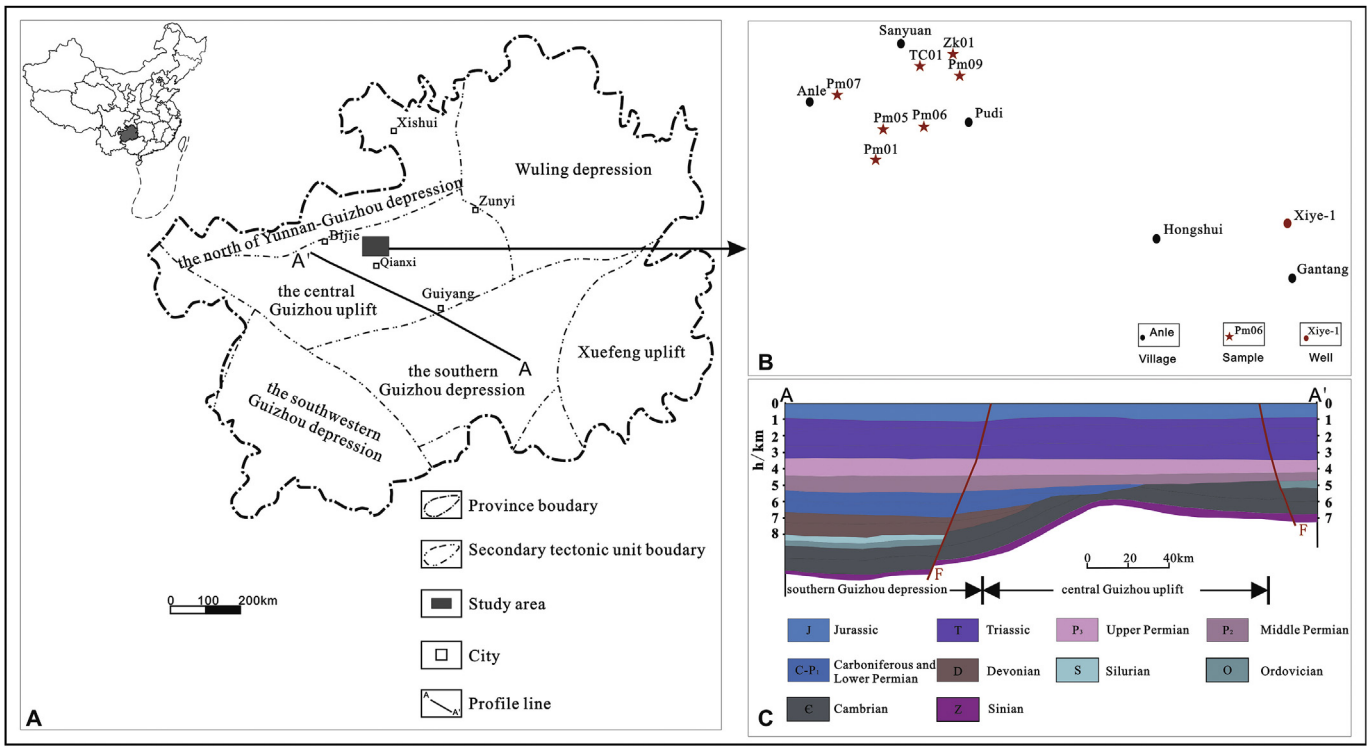

Fig. 1. (A) Location of the study area; (B) Distribution of the samples; (C) Regional tectonic profile.

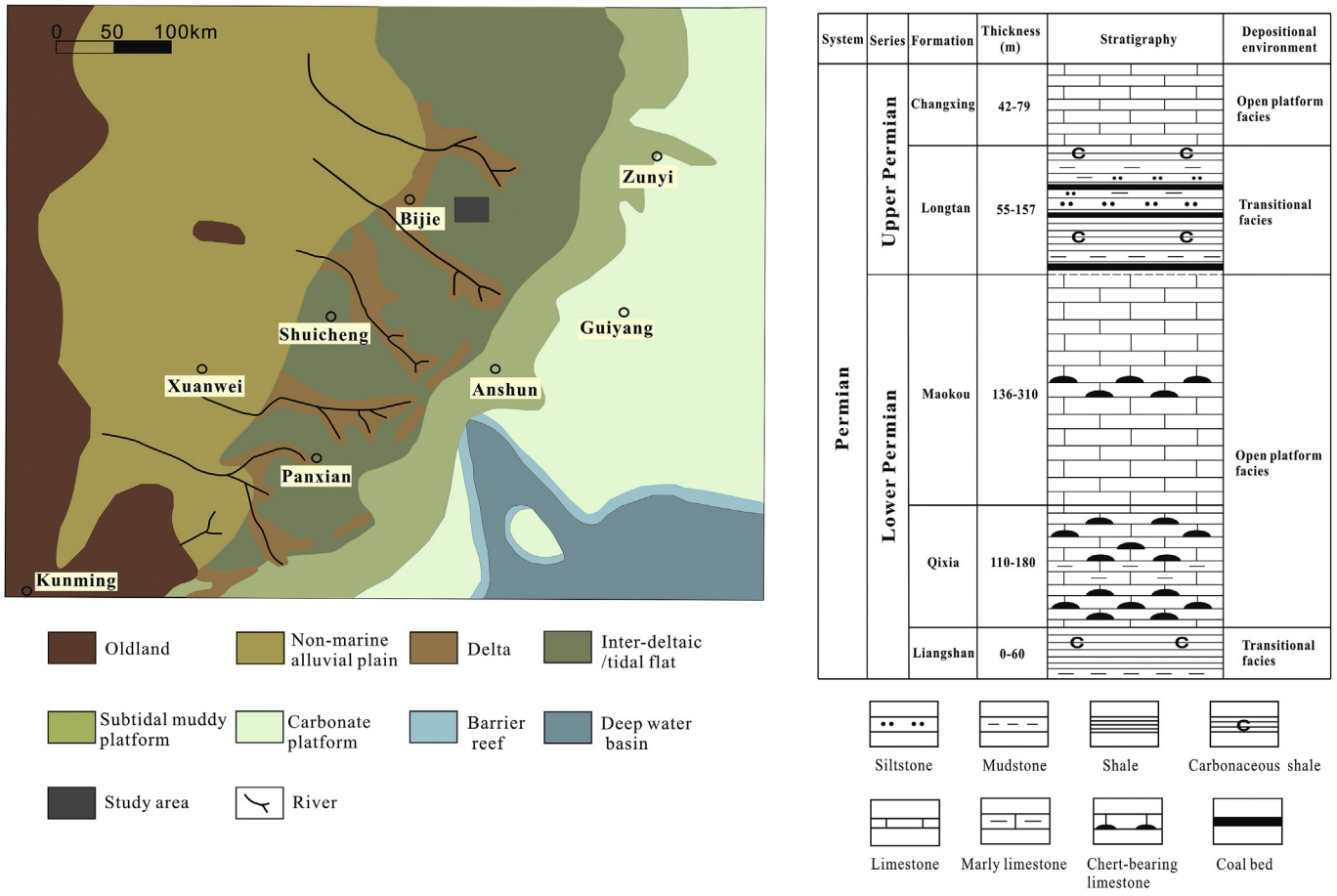

Fig. 2. (A) Palaeogeography map of late Permian sediment in the study area (modified from Shao et al., 1999); (B) Stratigraphic column of the Permian strata in the study area.

Table 1
TOC values, Rock-Eval pyrolysis data and Vitrinite Reflectance (Ro) data for the Longtan Formation samples.

Sample NO.	Sample type	TOC (%)	Ro (%)	S1 (mg/g)	S2 (mg/g)	Tmax°C	S1 + S2 (mg/g)	HI
PM01-99	outcrop	3.55	/	/	/	/	/	/
PM01-93	outcrop	5.37	/	0.018	0.15	499	0.17	2.84
PM01-92	outcrop	8.13	/	0.023	0.26	488	0.29	3.24
PM01-32	outcrop	2.07	/	0.015	0.08	501	0.09	3.74
PM05-48	outcrop	3.47	1.20	0.011	0.11	516	0.12	3.27
PM05-37	outcrop	24.70	/	0.026	0.38	498	0.41	1.54
PM05-36	outcrop	0.55	/	0.012	0.05	492	0.06	9.04
PM05-33	outcrop	2.10	1.12	0.010	0.09	495	0.10	4.10
PM05-31	outcrop	1.39	/	/	/	/	/	/
PM05-28	outcrop	1.23	/	0.010	0.07	491	0.08	5.56
PM06-53	outcrop	11.12	/	/	/	/	/	/
PM06-52	outcrop	5.41	/	0.016	0.30	576	0.31	5.51
PM06-51	outcrop	6.33	2.67	0.018	0.44	576	0.46	6.91
PM06-49	outcrop	7.90	/	/	/	/	/	/
PM06-38	outcrop	3.02	2.51	0.014	0.16	576	0.18	5.42
PM06-35	outcrop	1.91	/	0.013	0.28	450	0.29	14.46
PM06-32	outcrop	23.35	/	0.021	0.76	576	0.78	3.27
PM07-17	outcrop	0.84	1.10	0.014	0.06	497	0.07	6.98
PM07-13	outcrop	14.69	/	0.021	0.30	496	0.32	2.04
PM09-67	outcrop	26.99	/	0.025	0.98	576	1.01	3.65
PM09-66	outcrop	2.44	/	0.016	0.16	576	0.17	6.40
PM09-58	outcrop	5.99	/	0.019	0.34	576	0.36	5.61
PM09-56	outcrop	12.46	1.27	0.019	0.68	576	0.70	5.47
PM09-51	outcrop	2.76	/	0.018	0.26	473	0.28	9.39
PM09-27	outcrop	2.15	/	/	/	/	/	/
PM09-25	outcrop	2.16	/	0.014	0.16	576	0.17	7.25
PM09-23	outcrop	0.35	1.49	0.010	0.04	523	0.05	10.54
PM09-22	outcrop	2.03	1.67	0.022	0.08	479	0.10	3.89
PM09-19	outcrop	0.54	/	/	/	/	/	/
PM09-17	outcrop	0.45	/	0.014	0.05	577	0.06	10.76
PM09-16	outcrop	1.28	/	0.012	0.08	500	0.09	6.39
PM09-15	outcrop	0.65	/	0.023	0.05	576	0.07	6.98
PM09-11	outcrop	4.24	/	/	/	/	/	/
PM09-10	outcrop	1.91	2.44	0.032	0.09	576	0.12	4.64
PM09-09	outcrop	1.85	1.26	0.017	0.10	577	0.11	5.16
PM09-05	outcrop	5.30	/	0.013	0.18	576	0.19	3.39
TC01-29	outcrop	2.17	1.29	0.020	0.22	480	0.24	10.14
TC01-61	outcrop	1.16	1.15	0.020	0.11	484	0.13	9.48
ZK01-02	core	1.84	/	/	/	/	/	/
ZK01-05	core	9.47	2.74	0.019	0.70	576	0.72	7.44
ZK01-06	core	14.80	/	0.019	1.27	576	1.29	8.59
ZK01-07	core	3.27	2.07	0.013	0.26	570	0.27	7.89
ZK01-08	core	7.49	/	0.025	0.67	575	0.70	8.97
ZK01-09	core	4.93	/	0.016	0.26	576	0.28	5.36
ZK01-10	core	2.88	/	/	/	/	/	/
ZK01-11	core	1.54	/	/	/	/	/	/
ZK01-12	core	3.08	/	0.015	0.31	575	0.33	10.21
ZK01-14	core	2.68	/	/	/	/	/	/
ZK01-15	core	6.03	2.23	0.017	0.55	576	0.57	9.09
ZK01-16	core	1.29	1.89	0.016	0.13	576	0.15	10.13
ZK01-17	core	5.21	2.59	0.021	0.27	576	0.29	5.12
ZK01-18	core	6.24	/	0.017	0.50	576	0.52	8.09
ZK01-19	core	8.75	/	0.017	0.76	576	0.78	8.73
ZK01-20	core	4.38	2.14	0.018	0.37	575	0.39	8.43
ZK01-21	core	7.83	2.61	0.020	0.52	576	0.54	6.62
ZK01-22	core	3.21	/	/	/	/	/	/

TOC = total organic carbon; S1 = volatile hydrocarbon content (mg HC/g Rock); S2 = remaining hydrocarbon content (mg HC/g Rock); Tmax = temperature at maximum of S2 peak (°C); HI = hydrogen index (S2*100/TOC) (mg HC/g TOC).
"/" represent No data.

good shale gas resource potential (Fig. 3). Notably, in the 18 core samples, 83.3% of TOC values are greater than 2.0%, with an average of 5.27%. These showing that the Longtan shale met the source rock and shale reservoir criteria of high TOC.

For the samples from the well ZK01, the variation in TOC content with burial depth is shown in Fig. 4. The TOC values of Longtan shale varied greatly in the vertical direction. Such a trend is rarely observed for marine shales, such as the Longmaxi Formation shale, in which TOC usually decreases gradually from bottom to top. This is because the lithology of the Longtan Formation was significantly affected by the sedimentary environment of the transitional facies. The vertical variation of lithology is extremely complex, and the interactive appearance of shale, coal seam, silty shale, and siltstone occurs. Thus, the TOC values of the shale generally show high-value and low-value interactions. TOC values of some samples in thin coal seam even exceed 10%. As shown in Fig. 4, the corresponding shale thickness with TOC>2% is greater than 30 m, which implies that the Longtan shale may contain a considerable gas generation potential.

S1 + S2 is an index used to evaluate hydrocarbon generation potential. The S1 + S2 values for the Longtan shale vary from 0.06 to 1.29 mg HC/g rock (Table 1), with an average of 0.32 mg HC/g rock. It reveals that the Longtan shale has poor hydrocarbon generation

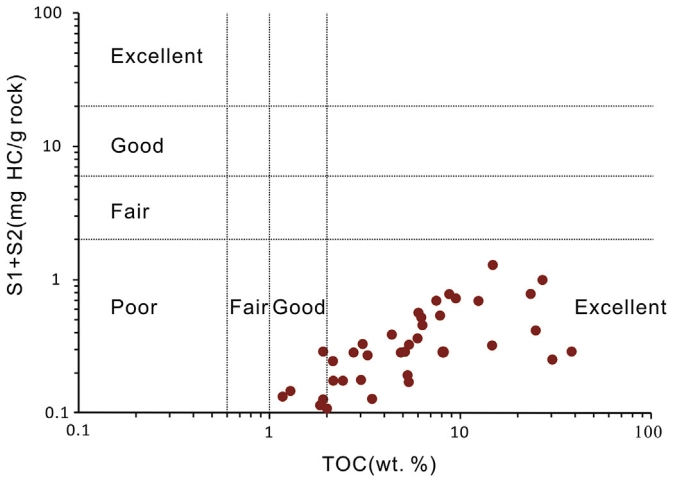

Fig. 3. Total hydrocarbon generation potential versus TOC plot for Longtan shale.

potential at present.

4.1.2. Thermal maturity

The thermal maturity is another important parameter for the evaluation of shale gas. It can affects not only gas generation potential, but also gas sorption capacity (Nie et al., 2009; Hui and Stephen, 2013). With the increase of thermal maturity, the gas generation potential decreases, but the gas sorption capacity increases. Vitrinite reflectance (Ro) and T_{max} are used to evaluate the maturation level of the Longtan shale in this work. Both core and outcrop samples have generally high Ro values in the range of 1.10–2.74%, with an average of 1.86%. There are 65% of samples having Ro values larger than 1.3%, and 45% of samples larger than 2%. Empirically, these high Ro values suggest that most of the Longtan shale samples are high-over matured and thermal maturity has been in the dry-gas window.

Furthermore, according to the Rock-Eval data from 46 shale samples, T_{max} values range from 450 °C to 576 °C, and most T_{max}

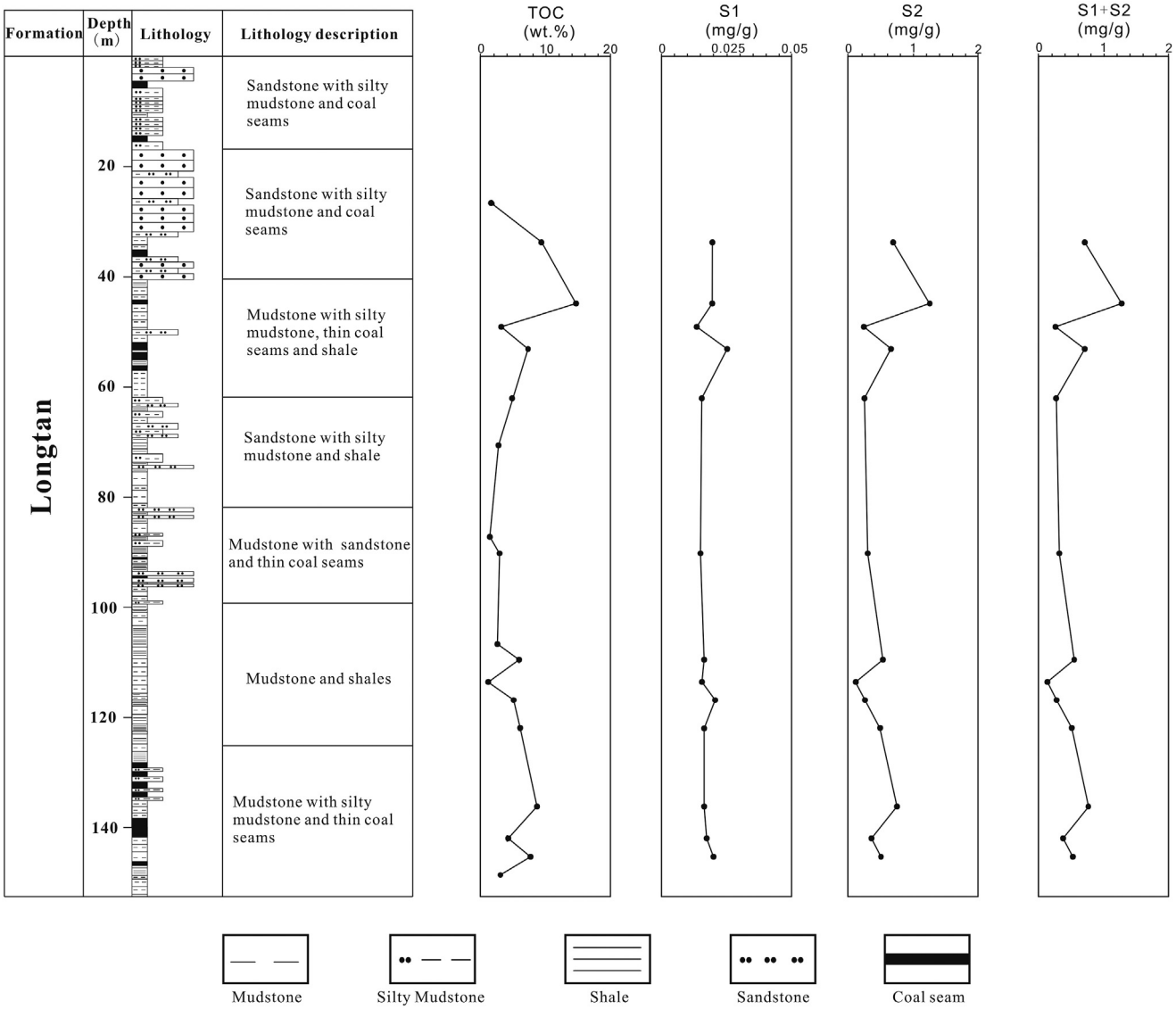

Fig. 4. Geochemical log column of the Zk01 well, including TOC, S1, S2, and S1 + S2.

values of the shale samples were >490 °C, indicating a high-over mature evolution stage. These data are consistent with the distribution of Ro values above. According to Peters (1986), T_{max} >470 °C marks the beginning of the wet gas window. It indicates that most of the Longtan shale samples fall in the gas window except for one sample, which had a T_{max} value of 450 °C.

The plot of total hydrocarbon generation potential versus TOC indicates that the Longtan shale currently has very low hydrocarbon generation potential (low S1 + S2) due to the high-over maturity. However, the high maturity and high remaining TOC indicate that the Longtan shale may be a good shale-gas reservoir in terms of the high amount of gas generated (see Fig. 5).

4.1.3. Organic matter type

Different organic matter types are derived from different types of primary production (i.e., algae or higher terrestrial plants) (Vandenbroucke and Largeau, 2007). In turn, the compositional characteristics of kerogen can provide insights into the changes in the depositional environment during sedimentation (Rimmer and Davis, 1988; Crosdale, 1993; Romero and Philp, 2012). The type of organic matter can not only determine the type of hydrocarbons generated from the shale, but also affect the hydrocarbon-generation behavior (Tissot et al., 1974; Chen, 2005). The type index (TI), which was calculated based on maceral compositions, indicates the organic matter type of Longtan shale was dominated by type III kerogen. Most Longtan shale samples are plotted at the center of the ternary diagram (Fig. 6). This result is consistent with a lagoon, swamp and delta environment of the Longtan shale, which indicates that the organic matter originated from higher plants. Thus, the type of hydrocarbon generated will be mainly gas during the whole maturity evolution phase.

4.2. Mineralogy

The sedimentary environment controls the mineral composition of shale, which can affect the pore characteristics and adsorption capacity, such as the pore size distribution (PSD), average pore size, porosity and specific surface area (SSA) (Bustin et al., 2009; Tan et al., 2014a, 2014b). The X-ray diffraction analyses of 27 shale samples indicate that clay minerals and brittle minerals (quartz, feldspar, and pyrite) are the major components of the Longtan Formation shale (Table 2), having average values of 56.69 wt% and

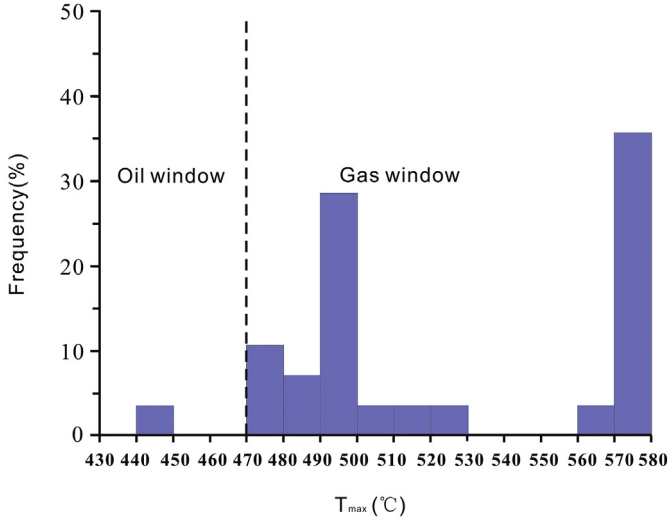

Fig. 5. Histograms of the T_{max} for the Longtan shale.

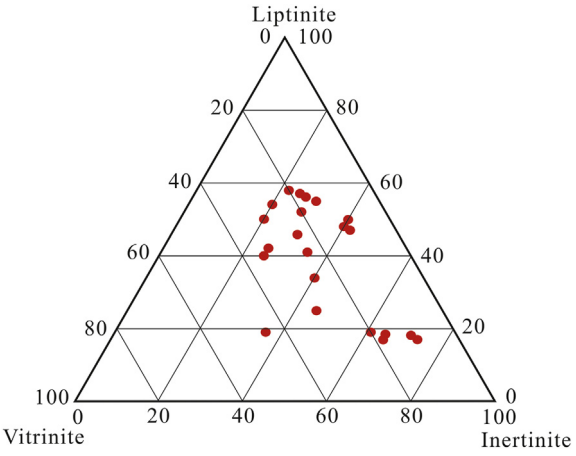

Fig. 6. Ternary diagram of maceral compositions of the Longtan shale.

40.28 wt%, respectively. Further analyses of clay minerals show that the mixed-layer illite-smectite (I/S) and illite are the main clay minerals. I/S, illite, chlorites and kaolinite have contents of 43.0%, 44.0%, 6.8% and 6.5%, respectively. Other minerals, including calcite, dolomite, pyrite and siderite can be observed in some shale samples, all with average contents <6 wt%.

The ternary diagram plotting mineralogy clearly shows that, compared to marine shales, the Longtan shale is poor in carbonate minerals and is relatively rich in clay minerals (Fig. 7). The mineral compositions of typical marine gas-bearing shales in North America (such as Barnett, Marcellus, Woodford and New Albany shale in the United States) are also shown in the ternary diagram. It shows that the Longtan shale is not similar to these marine shales in terms of mineral composition. In the ternary plot, more than 80% of the Longtan shale samples are located in the right zone, which represents the basic mineral compositions of transitional shales. In addition, the clay mineral contents were found to have a negative correlation with the quartz contents (Fig. 8). The variations in clay contents and quartz contents of the Longtan shale samples indicate that the amount and composition of deposited sediments varied significantly during the transport process, which reflects variations in the hydrodynamic conditions in the transitional sedimentary environment. Transitional shale also has a homogeneous clay composition. Illite and mixed illite/smectite are the dominant clay minerals in transitional shale, constituting 87% of the total clay minerals. The chlorite content in the Longtan transitional shale is significantly higher than that of marine shale. We believe this is due to the activity of Mount Emei basalt.

Rock mineral composition is very important for shale gas development. Previous studies have shown that clay content has a positive relationship with gas sorption capacity (Ross and Bustin, 2009; Guo et al., 2014). Clay minerals have larger surface area values compared to quartz and carbonates (Passey et al., 2010), which can enhance gas sorption capacity. Clay-rich shale, however, tends to be ductile and to deform instead of shattering. When hydraulic pressure and energy are injected into shales, fracture can hardly be successfully stimulated. However, the brittle mineral content can greatly affect matrix porosity and micro-fracture development, gas content, and fracturing stimulation pattern (Li et al., 2007; Zou et al., 2010; Sondergeld et al., 2010). Shale with higher brittle mineral content usually has a stronger ability to induce fractures, which are favorable for shale gas development. Sondergeld et al. (2010) suggested that shales with brittle mineral content greater than 40% and clay content less than 30% have commercial development potential.

Table 2
The mineral composition (wt. %) of the Longtan shale.

Sample NO.	I/%	K/%	C/%	I/S/%	Clay	Q	Fel.	Cal.	Dol.	Py.	Sid.	Bar.
PM01-93	33	4	6	57	69.4	25.1	5.5	/	/	/	/	/
PM01-92	31	37	7	25	69.8	9.0	21.2	/	/	/	/	/
PM01-32	45	0	2	53	66.3	30.9	0.0	/	/	/	/	2.8
PM01-30	67	16	0	17	69.1	21.1	9.8	/	/	/	/	/
PM05-48	39	4	12	45	55.1	28.4	16.5	/	/	/	/	/
PM05-37	32	17	0	51	31.4	62.0	6.6	/	/	/	/	/
PM05-33	85	0	12	3	55.7	26.9	15.9	/	/	/	/	1.5
PM05-28	61	0	35	4	61.9	24.7	13.4	/	/	/	/	/
PM06-52	54	4	8	34	68.9	8.0	17.3	/	/	/	/	5.8
PM06-51	33	5	10	52	70.8	21.3	6.4	/	/	/	1.5	/
PM06-39	39	29	4	28	62.2	29.4	8.4	/	/	/	/	/
PM06-38	53	2	3	42	52.4	22.0	22.3	/	/	/	/	3.3
PM06-32	73	0	2	25	43.2	45.6	8.2	/	/	3	/	/
PM07-17	45	0	1	54	71.8	22.5	5.7	/	/	/	/	/
PM09-58	38	2	6	54	74.9	18.3	6.8	/	/	/	/	/
PM09-56	48	0	16	36	39.8	51.8	8.4	/	/	/	/	/
PM09-51	46	0	7	47	65.0	17.0	17.0			1		/
PM09-16	32	0	1	67	77.2	14.3	8.5	/	/	/	/	/
PM09-15	38	0	1	61	68.9	21.9	9.2	/	/	/	/	/
PM09-09	41	0	1	58	50.0	22.0	24.0	/	/	/	/	4
ZK01-05	32	0	11	57	52.4	19.0	16.3	/	8.7	2.5	1.1	/
ZK01-07	38	0	8	54	44.0	24.1	17.1	/	8.4	2.9	3.5	/
ZK01-16	41	0	21	38	41.6	36.5	7.4	/	5.3	1	8.2	/
ZK01-17	53	39	6	2	62.0	16.7	8.4	2	5	5.6	/	/
ZK01-18	30	0	2	68	57.5	21.5	14.2	/	2.4	1.7	2.7	/
ZK01-20	33	0	4	63	53.0	24.0	11.0	/	6	2	4	/
ZK01-21	39	0	7	54	50.0	21.0	17.0	/	5	4	3	/

(I = illite, K = kaolinite, C = chlorite, I/S = mixed illite/smectite; these content refer to the proportion of the total clay minerals. Q = quartz, Fel. = feldspar, Cal. = calcite, Dol. = dolomite, Py. = pyrite, Sid. = siderite, and Bar. = barite).
"/" represent No data.

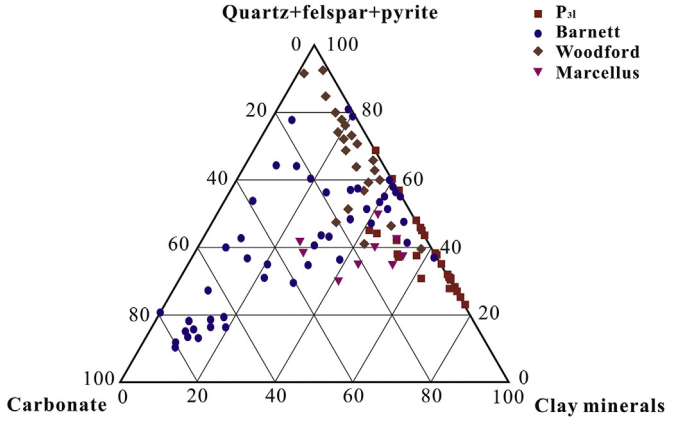

Fig. 7. Ternary diagram of the mineral composition for the Longtan shale (North American marine shale data provided by Ross and Bustin (2009), Gupta et al. (2013)).

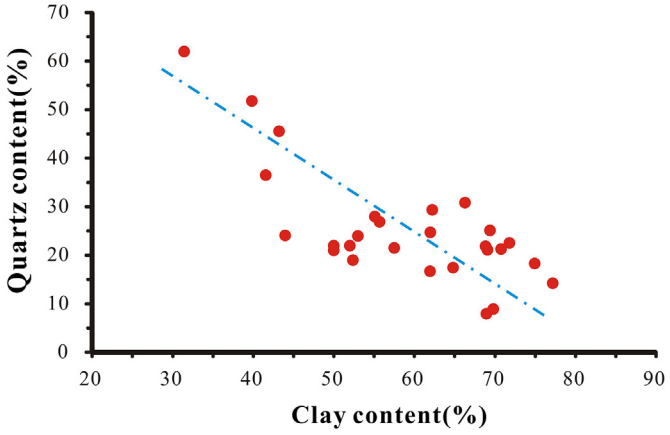

Fig. 8. Correlation between clay and quartz content.

4.3. Microscopic pore types

Porosity is an important parameter to reflect the storage capacity. Though the potential of gas generation in high quality shale is great, the potential productivity is likely low in part of this section with low storage capacity. Our measurements show that the Longtan shale has porosity in the range of 1.39%–5.05% (2.42% on average) and permeability in the range of 0.025–1.11 $\times$ 10^{-3} mD (0.573 $\times$ 10^{-3} mD on average). As lower limits of porosity and permeability for shale gas reservoir have been respectively suggested as 1% and 0.001 mD (Nie et al., 2009), it seems that the Longtan shale have a relatively good properties for potential exploration. Based on previous studies on pore classification (Zou et al., 2010; Loucks et al., 2012), pores can be divided into interparticle (interP) pores, intraparticle (intraP) pores, organic matter (OM) pores, and microfractures. SEM observation revealed that intraP pores, interP pores, and microfractures are developed well in the Longtan shale, while OM pores are less developed.

4.3.1. OM pores

OM pores result from the generation of oil and gas with increasing thermal maturity (Loucks et al., 2009, 2012; Mastalerz et al., 2013). Loucks et al. (2012) suggested that OM pores begin to develop when Ro is at least 0.6%. The vitrinite reflectances of the Longtan shale all exceed 1.0%, which is sufficiently high for pore development in OM. However, OM pores are extremely rare or absent in the Longtan shale samples based on the analysis of SEM images. The rarity of OM pores should be due to the organic type (type-III kerogen). This is because little liquid hydrocarbons can be generated by vitrinite and inertinite. Therefore, very few organic

pores can be formed during thermal maturation.

4.3.2. IntraP pores

IntraP pores are the major contributor to porosity in the Longtan shale. Three types of intraP pores are dominant: dissolution pores, intraP pores within clay particles, and inter-crystalline pores within pyrite framboids. Dissolution pores are generated from the partial dissolution of particles, which may be due to the increase of burial depth, change of temperature, and pressure or the corrosive fluids. Fig. 9 demonstrates that the dissolution pores can be developed in feldspar grains. Dissolution pores are well developed in feldspar particles and have irregular shapes and large size in the range of 3–20 μm (Fig. 9A). IntraP pores within clay particles are mainly developed in illite, which is very small owing to the distortion of the particles during compaction (Fig. 9B). Inter-crystalline pores within pyrite framboids are common intra-particle pores in the Longtan shale, with pore diameters ranging from 10 nm to 600 nm (Fig. 9C). These pores may significantly contribute to the connectivity after fracturing.

4.3.3. InterP pores

InterP pores are abundant in the Longtan shale and connect well with each other. InterP pores occur between grains, such as quartz and clay particles. They mainly occur as irregular between illite, with sizes in the range of 5–20 μm (Fig. 9D). Owing to the effect of burial compaction, the particles have some deformation, which has good directionality. These pores easily close during compaction because of the strong plastic deformation of clay, which would destroy the connectivity. Others are observed as triangular, oval or irregular between particles, and range in size from tens of nanometers to hundreds of nanometers (Fig. 9E and F).

4.3.4. Microfractures

Microfractures are abundant in the Longtan shale, which can significantly provide permeable pathways. Microfractures are developed mainly in brittle minerals (Fig. 9G, H, I), and they are elongated and range in size from several to tens of microns in length and range from 2 to 5 μm in width. Some clay-rich samples show many fractures, and the fractures are oriented in a certain direction. These traits are considered artifacts formed during sample preparation.

Dissolution pores in feldspar particles. (B) IntraP pores within illite. (C) Inter-crystalline pores within pyrite framboids. (D) InterP pores in illite. (E) Irregularly shaped interP pores. (F) InterP pores in clay mineral. (G) Microfractures in clay mineral. (H) Same as G. (F) Microfractures in brittle mineral.

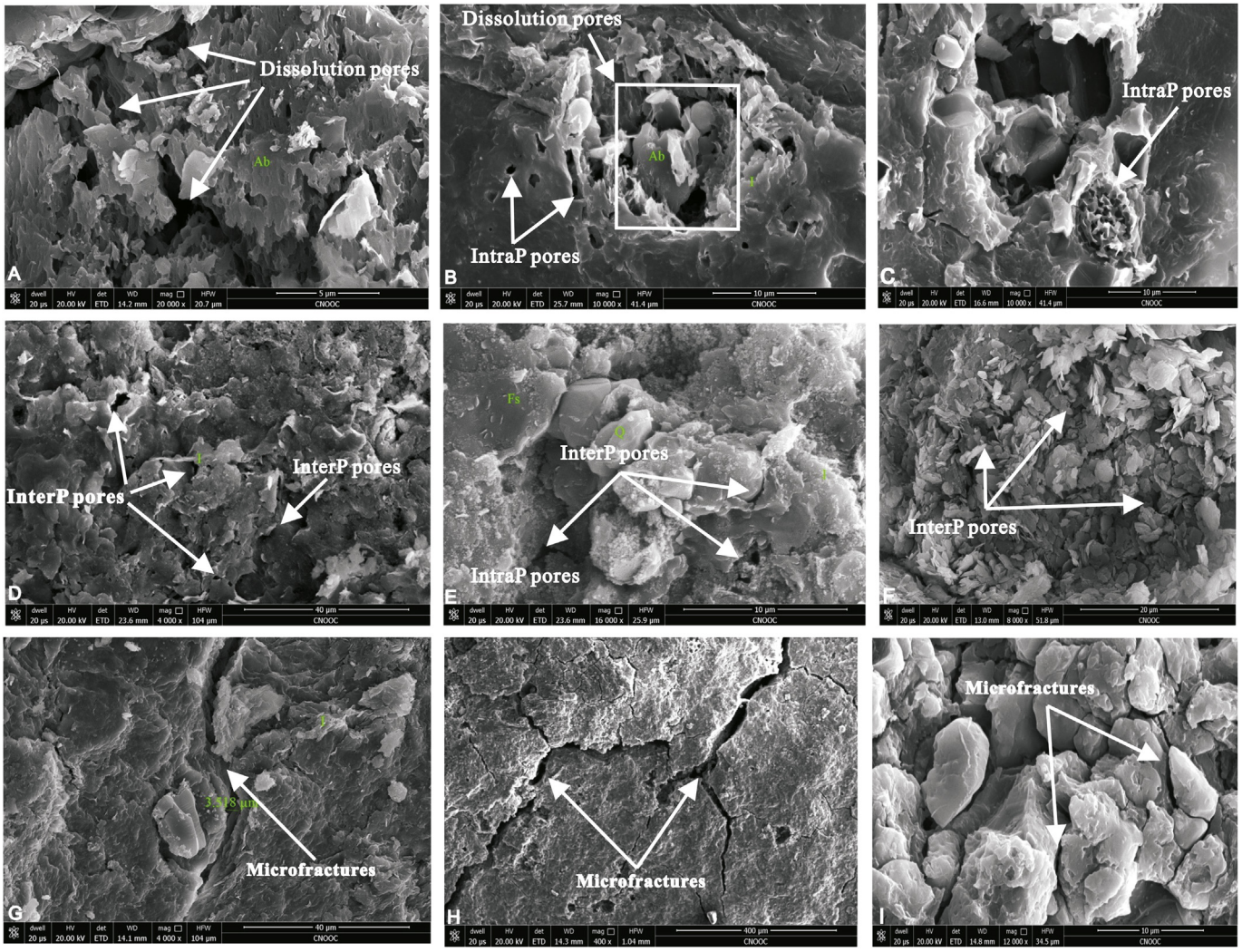

Fig. 9. Scanning electron microscope (SEM) images of the Longtan shale. WD = working distance; det = detector; mag = magnification; HV = high voltage (accelerating voltage); HFW = horizontal frame width; BSED = backscattered electron detector.

Table 3
Key parameters of major gas shale in America and the Longtan shale.

Shale name	Basin	Age	Depositional setting	Burial depth(m)	TOC(%)	Ro (%)	Kerogen type	Porosity (%)
Barnett	Fort Worth	Mississippian	Marine	1981~2591	2.0~7.0	1.1~2.2	II	4~5
Ohio	Appalachian	Devonian	Marine	610~1524	0.5~4.7	0.4~1.3	I-II	4.7
Antrim	Michigan	Devonian	Marine	183~730	1.0~20.0	0.4~0.6	I	9
New Albany	Illinois	Devonian	Marine	183~1494	1~25.0	0.4~1.0	II	10~14
Lewis	San Juan	Cretaceous	Transitional	914~1829	0.45~2.5	1.6~1.88	I	3.0~5.5
Longtan	–	Permian	Transitional	1300~2500	0.35~26.99	1.1~2.74	III	1.39~5.05

5. Comparison of the properties of the Longtan shale and other marine shale

The Longtan shale was deposited on a lagoon, swamp and delta environment, which leads to the stratigraphic facies of the transitional shale change rapidly, and it is often interbedded with coal, sandstone and limestone of low thickness. Table 3 lists key parameters of the five famous gas shale in America and the Longtan shale. The shale gas potential of the Longtan shale are suggested by its high TOC content and the high maturity. Commercially exploited marine shale in the United States is dominated by type I-II kerogen. However, the organic matter type of the Longtan Formation shale was dominated by type III kerogen, which is more conducive to the formation and accumulation of shale gas. The transitional shale has very low permeability compared to marine shale in United states, which is probably due to high content of compactible clay.

In summary, high TOC value, high thermal maturity level, and moderate burial depth are favorable factors for shale gas exploration prospect. However, the high clay content of transitional shale can bring about a challenge for shale-gas exploration and development due to its low brittleness during hydrofracturing.

6. Conclusions

(1) The Longtan shale has high TOC value (5.34% in average)and high thermal maturation level (Ro 1%–2.74%), with OM present type-III kerogens, which are favorable for generating shale gas. Ro and T_{max} data indicate that the Longtan shale is at a high maturity stage and has entered the gas window. High maturity and high remaining TOC indicate that the Longtan shale has generated significant amounts of gas and can be a good shale gas reservoir.
(2) The XRD results show that the Longtan shale has a high clay mineral content, illite and I/S mix layers are the dominant clay minerals, brittle minerals are of low content, and carbonates are rare or absent.
(3) Based on SEM observations, interP pores, intraP pores, and microfractures are developed well in Longtan shale, but OM pores are rarely developed. IntraP pores and microfractures are considered to provide space for gas storage and migration.
(4) High TOC value, high thermal maturity level, and moderate burial depth are favorable factors for shale gas exploration in the Longtan shale. However, the high clay content of the transitional shale may be unfavorable for shale-gas exploration and development.

Acknowledgements

The authors thank the Keyuan Engineering Testing Center of Sichuan province for help with the analysis of organic geochemical characteristics. The authors extend special thanks to Michael Abrams at the Imperial College, London for help with geochemistry analyses and useful comments. The authors also wish to thank anonymous reviewers for their highly constructive reviews.

References

Behar, F., Beaumont, V., Penteado, H.D.B., 2001. Rock-Eval 6 technology: performances and developments. Oil Gas Sci. Technol. 56 (2), 111–134.
Bowker, K.A., 2007. Barnett shale gas production, fort worth basin: issues and discussion. AAPG Bull. 91 (4), 523–533.
Bustin, R.M., Bustin, A., Ross, D., Chalmers, G., Murthy, V., Laxmi, C., Cui, X., 2009. Shale gas opportunities and challenges. Search Discov. 20–23. Articles 40382.
Chen, Z.N., 2005. Petroleum and Natural Gas Geology. Geology Press, pp. 143–151.
Crosdale, P.J., 1993. Coal maceral ratios as indicators of environment of deposition: do they work for ombrogenous mires? An example from the Miocene of New Zealand. Org. Geochem. 20 (6), 797–809.
Curtis, J.B., 2002. Fractured shale-gas systems. AAPG Bull. 86 (11), 1921–1938.
Dang, W., Zhang, J.C., Tang, X., Chen, Q., Han, S.B., Li, Z.M., Du, X.R., Wei, X.L., Zhang, M.Q., Liu, J., Peng, J.L., Huang, Z.L., 2015. Shale gas potential of Lower Permian marine-continental transitional black shales in the southern North China Basin, Central China: characterization of organic geochemistry. J. Nat. Gas Sci. Eng. 28, 639–650.
Dou, X.Z., Jiang, B., Qin, Y., Wang, W., Chen, W.Y., 2012. Structure evolution in west of Guizhou area and control to seam in Late Permian. Coal Sci. Technol. 40 (3), 109–114.
Gai, S.H., Liu, H.Q., He, S.N., Mo, S.Y., Chen, S., Liu, R.H., Huang, X., Tian, J., Lv, X.C., Wu, D.X., He, J.L., Gu, J.R., 2016. Shale reservoir characteristics and exploration potential in the target: a case study in the Longmaxi Formation from the southern Sichuan Basin of China. J. Nat. Gas Sci. Eng. 31, 86–97.
Gao, J., Liu, G.D., Yang, W.W., Zhao, D.R., Chen, W., Liu, L., 2016. Geological and geochemical characterization of lacustrine shale, a case study of Lower Jurassic Badaowan shale in the Junggar Basin, Northwest China. J. Nat. Gas Sci. Eng. 31, 15–27.
Guo, H.J., Jia, W.L., Peng, P.A., Lei, Y.H., Luo, X.R., Cheng, M., Wang, X.Z., Zhang, L.X., Jiang, C.F., 2014. The composition and its impact on the methane sorption of lacustrine shales from the Upper Triassic Yanchang Formation, Ordos Basin, China. Mar. Petrol. Geol. 57 (2), 509–520.
Guo, T.L., Liu, R.B., 2013. Implications from marine shale gas exploration breakthrough in complicated structural area at high thermal stage: taking Longmaxi Formation in well JY1 as an example. Nat. Gas. Geosci. 24 (4), 643–651.
Gupta, N., Rai, C.S., Sondergeld, C.H., 2013. Integrated petrophysical characterization of the Woodford shale in Oklahama. Petrophysics 54 (4), 1–35.
He, J.X., Duan, Y., Zhang, X.L., Wu, B.X., Xu, L., 2011. Hydrocabon generation conditions of the shale in Niutitang Formation of lower Cambrian, southern Chongqing and northern Guizhou. Mar. Geol. Front. 27 (3), 34–40.
Hui, J., Stephen, A.S., 2013. Characterization for source rock potential of the bakken shales in the williston basin, North Dakota and Montana. In: Unconventional Resources Technology Conference, vol. 168788. SPE, pp. 1–10.
Hunt, M., 1979. Petroleum Geochemistry and Geology. W. H. Freeman and Company.
Jarvie, D.M., Hill, R.J., Ruble, T.E., Pollastro, R.M., 2007. Unconventional shale-gas systems: the Mississippian Barnett Shale of north-central Texas as one model for thermogenic shale-gas assessment. AAPG Bull. 91 (4), 475–499.
Jiang, S., Xu, Z.Y., Feng, Y.L., Zhang, J.C., Cai, D.S., Chen, L., Wu, Y., Zhou, D.S., Bao, S.J., Ju, Y.W., Wang, G.C., Bu, H.L., Li, Q.G., Yan, Z.F., 2014. China organic-rich shale geologic features and special shale gas production issues. J. Rock Mech. Geotech. Eng. 6 (3), 196–207.
Li, J., Yu, B.S., Zhang, J.C., Li, Y.X., Wu, J.S., 2012. Reservoir characteristics and their influence factors of the Lower Cambrian dark shale in northern Guizhou. Oil Gas Geol. 33 (3), 364–374.
Li, X.J., Hu, S.Y., Cheng, K.M., 2007. Suggestions from the development of fractured shale gas in North America. Petrol. Explor. Dev. 34 (4), 392–400.
Loucks, R.G., Reed, R.M., Ruppel, S.C., Jarvie, S.C., 2009. Morphology, genesis, and distribution of nanometer-scale pores in siliceous mudstones of the Mississippian Barnett shale. J. Sediment. Res. 79 (12), 848–861.
Loucks, R.G., Reed, R.M., Ruppel, S.C., Hammes, U., 2012. Spectrum of pore types and networks in mudrocks and a descriptive classification for matrix-related mudrock pores. AAPG Bull. 96 (6), 1071–1098.
Mastalerz, M., Schimmelmann, A., Drobniak, A., Chen, Y., 2013. Porosity of Devonian and Mississippian New Albany Shale across a maturation gradient: insights from organic petrology, gas adsorption, and mercury intrusion. AAPG Bull. 97, 1621–1643.
Nie, H.K., Tang, X., Bian, R.K., 2009. Controlling factors for shale gas accumulation and prediction of potential development area in shale gas reservoir of South China. Acta Pet. Sin 30 (4), 484–491.
Niu, X.S., Feng, C.M., Liu, J., 2007. Formation mechanism and time of Qianzhong

uplift. Mar. Orig. Petrol. Geol. 12 (2), 46–50.
Passey, Q.R., Bohacs, K.M., Esch, W.L., Klimentidis, R., Sinha, S., 2010. From oil-prone source rock to gas-producing shale reservoir-geologic and petrophysical characterization of unconventional shale-gas reservoirs. SPE-131350. In: CPS/SPE International Oil & Gas Conference and Exhibition in China. June 8–10, Beijing, China.
Peters, K.E., 1986. Guidelines for evaluating petroleum source rock using programmed pyrolysis. AAPG Bull. 70 (3), 318–329.
Rimmer, S.M., Davis, A., 1988. The influence of depositional environments on coal petrographic composition of the Lower Kittaning Seam, western Pennsylvania. Org. Geochem. 12 (4), 375–387.
Romero, A.M., Philp, R.P., 2012. Organic geochemistry of the Woodford Shale, southeastern Oklahoma: how variable can shales be? AAPG Bull. 96 (3), 493–517.
Ross, D.J.K., Bustin, R.M., 2009. The importance of shale composition and pore structure upon gas storage potential of shale gas reservoirs. Mar. Petrol. Geol. 26 (6), 916–927.
Shao, L., Hao, L., Yang, L., Zhang, P., Tian, B., 1999. High resolution sequence stratigraphy of the Late Permian coal measures in southwestern China. In: Xie, H., Golosinski, T.S. (Eds.), Mining Science and Technology 99. Balkema, Rotterdam, pp. 239–242.
Sondergeld, C.H., Newsham, K.E., Comisky, J.T., Rice, M.C., Rai, C.S., 2010. Petrophysical Considerations in Evaluating and Producing Shale Gas Resources. SPE Unconventional Gas Conference, Pittsburgh.
Tan, J.Q., Horsfield, B., Fink, R., Krooss, B., Schulz, H.M., Rybacki, E., Tocher, B.A., Zhang, J.C., Boreham, C.J., Graas, V.G., Tocher, B.A., 2014b. Shale gas potential of the major marine shale formations in the UpperYangtze Platform, South China, Part III: mineralogical, lithofacial, petrophysical, and rock mechanical properties. Energy & Fuels 28 (2), 2322–2342.
Tan, J.Q., Weniger, P., Krooss, B., Merkel, A., Horsfield, B., Zhang, J.C., Boreham, C.J., Graas, V.G., Tocher, B.A., 2014a. Shale gas potential of the major marine shale formations in the Upper Yangtze Platform, South China, Part II: methane sorption capacity. Fuel 129, 204–218.
Tang, X., Zhang, J.C., Wang, X.Z., Yu, B.S., Ding, W.L., Xiong, J.Y., Yang, Y.T., Wang, L., Yang, C., 2014. Shale characteristics in the southeastern Ordos Basin, China: implications for hydrocarbon accumulation conditions and the potential of continental shales. Int. J. Coal Geol. 128, 32–46.
Tissot, B., Durand, B., Espitalie, J., Combaz, A., 1974. Influence of nature and diagenesis of organic matter in formation of petroleum. AAPG Bull. 58 (3), 499–506.
Vandenbroucke, M., Largeau, C., 2007. Kerogen origin, evolution and structure. Org. Geochem 38 (5), 719–833.
Wang, Z.P., Zhang, J.C., Sun, R., Liu, C.W., Du, X.R., Lu, Y.Y., 2015. The gas-bearing characteristics analysis of the Longtan Formation transitional shale in Well Xiye 1. Earth Sci. Front. 22 (2), 243–250.
Zhang, J.C., Jiang, S.L., Tang, X., Zhang, P.X., Tang, Y., Jin, T.Y., 2009. Accumulation types and resources characteristics of shale gas in China. Nat. Gas. Ind. 29 (12), 109–114.
Zhang, J.C., Xu, B., Nie, H.K., Wang, Z.Y., Lin, T., 2008. Exploration potential of shale gas resource in China. Nat. Gas. Ind. 28 (6), 136–140.
Zhao, Z.H., Zhang, G.Q., Xue, X.L., 2008. Fossil oil pools and residual oil and gas pools in the lower assemblage of Qianzhong uplift. Nat. Gas. Ind. 28 (8), 39–42.
Zou, C.N., Dong, D.Z., Wang, S.J., Li, J.Z., Li, X.J., Wang, Y.M., Li, D.H., Chen, K.M., 2010. Geological characteristics, formation mechanism and resource potential of shale gas in China. Pet. Explor. Dev. 37 (06), 641–653.